Biomolecules and Biomedicine

ISSN: 2831-0896 (Print) | ISSN: 2831-090X (Online)

Journal Impact Factor® (2024): 2.2

CiteScore® (2024): 5.2

www.biomolbiomed.com | blog.bjbms.org

The BiomolBiomed publishes an "Advanced Online" manuscript format as a free service to authors in order to expedite the dissemination of scientific findings to the research community as soon as possible after acceptance following peer review and corresponding modification (where appropriate). An "Advanced Online" manuscript is published online prior to copyediting, formatting for publication and author proofreading, but is nonetheless fully citable through its Digital Object Identifier (doi®). Nevertheless, this "Advanced Online" version is NOT the final version of the manuscript. When the final version of this paper is published within a definitive issue of the journal with copyediting, full pagination, etc., the new final version will be accessible through the same doi and this "Advanced Online" version of the paper will disappear.

RESEARCH ARTICLE

Shi et al: KDM3A drives NSCLC growth and metastasis

KDM3A drives NSCLC proliferation and metastasis via H3K9 demethylation, EMT activation and MMP-9 upregulation

Bingqing Shi^{1,3}, Zhe Wang², Lei Xiu¹, Luyao Li¹, Xiaolian Yang¹, Guanhua Wang¹, Jianjun Li¹, Hu Wang¹, Yuning Han^{3*}

¹Department of Cardio-Thoracic Surgery, General Hospital of Ningxia Medical University, Yinchuan, China;

²Anesthesiology Department, Yinchuan Hospital of Traditional Chinese Medicine, Yinchuan, China;

³Department of General Thoracic Surgery, General Hospital of Ningxia Medical University, Yinchuan, China.

*Correspondence to Yuning Han: nxhyuning@163.com.

DOI: https://doi.org/10.17305/bb.2025.11251

ABSTRACT

Histone methylation dysregulation is a crucial epigenetic driver of lung carcinogenesis; however, the role of lysine-specific demethylase 3A (KDM3A) in non-small cell lung cancer (NSCLC) remains inadequately understood. In this study, we established NSCLC cell models with both KDM3A overexpression and knockdown to investigate its functional impact. In vitro assays demonstrated that KDM3A depletion increased histone H3 lysine 9 dimethylation (H3K9me2), suppressed cell proliferation, and impaired migration and invasion by attenuating epithelial-mesenchymal transition (EMT) and the expression of matrix metalloproteinase-9 (MMP-9). Conversely, KDM3A overexpression led to reduced H3K9me2 levels, activated EMT, and enhanced metastatic potential. Mechanistically, KDM3A decreased H3K9me2 occupancy at the promoters of VIM and MMP-9, thus upregulating their expression. Additionally, KDM3A downregulated E-cadherin by activating the p-STAT3 pathway. In vivo, KDM3A knockdown significantly inhibited tumor growth in xenograft models. Clinical analyses revealed elevated KDM3A expression in metastatic NSCLC tissues, with a negative correlation between KDM3A and H3K9me2, and a positive association between KDM3A and FOXP3. These findings establish KDM3A as an epigenetic modulator of NSCLC progression through H3K9me2-dependent regulation of EMT and metastatic pathways, highlighting its therapeutic potential for NSCLC treatment.

Keywords: Demethylation, non-small cell lung cancer, epithelial-mesenchymal transition, cell invasion, cell proliferation, KDM3A.

INTRODUCTION

Lung cancer is the leading cause of cancer-related death worldwide and is often categorized as either non-small cell lung cancer (NSCLC) and small cell lung cancer (SCLC). Despite encouraging developments in lung cancer treatments, NSCLC accounts for more than 75% of all lung cancer cases. A comprehensive understanding of the molecular mechanisms underlying NSCLC is therefore crucial for identifying more effective prevention and therapeutic strategies.

Lung cancer is the most common malignant tumor. It is often categorized as either non-small cell lung cancer (NSCLC) or small cell lung cancer (SCLC), with NSCLC accounting for 80–85% of all cases [1, 2]. Nonetheless, investigating the mechanisms and therapeutic strategies for lung cancer progression remains a critical concern. For early NSCLC diagnosis and tailored therapy, a thorough investigation of putative disease indicators and targeting molecules is necessary. The swift progress in epigenetic research has advanced our understanding of lung cancer pathogenesis and contributed to personalized lung cancer treatment [3, 4]. Epigenetic mechanisms, which encompass post-translational modifications of DNA and histones that impact chromatin structure, govern gene expression in normal development and play a role in carcinogenesis and cancer progression [5, 6].

In eukaryotic cells, the epigenetic control of gene expression occurs primarily through post-translational modifications and DNA methylation changes of the core histones' N-terminal tails. The nature and genomic location of these modifications directly influence chromatin accessibility and readability [7-9]. One key modification is histone methylation, a rapidly advancing field of research, whose dynamic regulation plays a critical role in influencing transcription [10].

KDM3A is an epigenetic activator that involved in regulating gene expression by removing H3K9me2 modifications. While KDM3A as been implicated in tumor progression in various cancers, its specific function and molecular mechanism in NSCLC remain unclear and require further investigation. The methylation of histone H3 lysine 9 (H3K9) is a fundamental epigenetic mark essential for heterochromatin formation and the regulation of diverse biological processes, including gene silencing [11, 12]. As an eraser of H3K9me2, KDM3A can profoundly influence cellular function by dysregulating gene expression programs [13-15]. Genetic ablation or mis-

targeting of a single H3K9 methyltransferase can lead to impaired cell differentiation, loss of tissue properties, premature senescence, and cancer [16]. Supporting its protumorigenic role[17], KDM3A knockdown has been shown to suppress the invasive and migratory capacity of cancer cells in multiple contexts, including breast cancer [18], abdominal aortic aneurysms [15], clear cell renal cell carcinoma [18], abdominal aortic tumor[19], and glioblastoma [20, 21].

However, a comprehensive understanding of the H3K9 methylation regulator KDM3A in NSCLC, particularly its underlying molecular mechanisms, is yet to be explored.

In this study, we investigated the role of KDM3A in the proliferation and migration of NSCLC cells both *in vitro* and *in vivo*. We assessed the impact of KDM3A on H3K9me2 levels via western blot. Furthermore, we conducted a detailed analysis of how KDM3A influence genes associated with cell migration and invasion using a combination of techniques, including western blot, qRT-PCR, chromatin immunoprecipitation (ChIP), wound healing, trans-well assays and xenograft models. Finally, we evaluated the expression of KDM3A in clinical NSCLC samples by immunohistochemistry (IHC) staining. These findings provide new insights into KDM3A as a potential target for NSCLC therapy and underscore the importance of further investigating its role in tumor progression.

MATERIALS AND METHODS

Cell culture

The NSCLC cell lines (A549, H1299 and HCC827) utilized in this investigation came from ATCC (Manassas, VA, USA), respectively. Cells were authenticated and tested as microplasm free using PCR kit (Beyotime Biotechnology Co., Cat# C0301S, Shanghai, China). H1299 and HCC827 cells were cultured with Roswell Park Memorial Institute 1640 (RPMI-1640) medium (Gibco, C11875500BT, Beijing, China), A549 cells were grown using Dulbecco's Modified Eagle Medium (DMEM) elevated glucose medium (Hyclone, SH30284.01, Shanghai, China), supplemented with 10% fetal bovine serum (FBS) (Cytiva, SH30406.05, Taurange, New Zealand) and supplemented with 100U/ml Penicillin-Streptomycin Solution (Gibco, 10378016, CA, USA). Histone demethylase inhibitor IOX1 was abtained from Medchemexpress

(Cat# HY-12304). CBA-1 was obtained from ProbeChem (Cat# PC-20353). Cisplatin was obtained from Medchemexpress (Cat# HY-17394).

Quantitively reverse transcription PCR (qRT-PCR)

Standard techniques with Trizol reagents (Sigma-Aldrich; T9424; Germany.) were used to extract RNA from cells. Following a 10-minute lysing period and a 15-minute centrifugation at 12,000 g, the samples were exposed to isopropanol treatment. After that, the extracted RNA was reverse transcribed into complementary DNA (cDNA) through the PrimeScript RT kit (Takara Holdings Inc; RR047Q; Kyoto, Japan). Quantitively reverse transcription PCR (qRT-PCR) was carried out using the TB Green@Premix Ex TaqTM II (Takara; CN830S; Beijing, China) guidelines using an Applied Biosystems, Inc. (Carlsbad, CA, USA) 7500 system. The primers in both forward and reverse for human KDM3A were 5'-

GCCAACATTGGAGACCACTTCTG-3' and 5'-

CTCGAACACCTTTGACAGCTCG-3'. Human E-cadherin (CDH1), forward: 5'-

GCCTCCTGAAAAGAGAGTGGAAG-3', reverse:5'-

TGGCAGTGTCTCCCAAATCCG-3', human Vimentin (VIM), forward: 5'-

AGGCAAAGCAGGAGTCCACTGAA-3', reverse: 5'-

ATCTGGCGTTCCAGGGACTCAT-3', human MMP9, forward:5'-

GCCACTACTGTGCCTTTGAGTC-3', reverse: 5'-

CCCTCAGAGAATCGCCAGTACT-3', human KDM3B, forward: 5' -

GCTCGTAATGTCTGAGAAGGAGG-3', reverse: 5'-

CACATTTGCGACAAACCCAGTGG-3'; human KDM3C, forward: 5'-

TCCTGTCAGACCTTCCAGTGCA-3', reverse: 5' -

GTGGATGCAACAGACCGTAATGG-3', human Actin, forward: 5'-

CACCATTGGCAATGAGCGGTTC-3', reverse: 5'-

AGGTCTTTGCGGATGTCCACGT-3'.

Western Blot

Total protein was obtained from the samples using RIPA lysis buffer (Beyotime Biotechnology Co., G3424; Shanghai, China). Pierce™ BCA Protein Assay Kit (Thermo Fisher, Cat#23227) was utilized to quantify the protein specimens. Proteins were separated using SDS-PAGE electrophoresis, then transferred to a polyvinylidene fluoride (PVDF) membrane (Biorad, 1620177, Shanghai, China). Following an hour

at room temperature blocking the membranes with 5% non-fat milk, membranes were washed with 1 × TBST (Tris: 20mM, NaCl: 150mM, Tween® 20 detergent: 0.1% (w/v)) for three times, incubated with antibodies against KDM3A (GeneTex, 54313, 1:1000), KDM3B (Proteintech, 19915-1-AP, 1:1000), H3K9me2 (Cell signaling technology, 4658T, 1:2000), β-actin (Santa Cruz Biotechnology, sc-47778, 1:1000), MMP-9 (Santa Cruz Biotechnology, sc-393859, 1:1000), E-cadherin (Santa Cruz Biotechnology, sc-8426,1:1000), Vimentin (Santa Cruz Biotechnology, sc-6260, 1:1000), FAK (Cell Signaling Technology, 3285S, 1:1000), pFAK (Tyr397) (Cell Signaling Technology, 3283, 1:1000), STAT3 (Cell signaling Technology, 4904, 1:1000), pSTAT3 (Y705) (Cell Signaling Technology, 9131, 1:1000), GAPDH (Proteintech, HRP-60004,1:5000) overnight at 4°C, washed for three times utilizing 1 ^x TBST and subsequently incubated for 1 hour with HRP-labeled secondary antibody in room temperature, respectively (ab205718 for anti-Rabbit, ab20571 for anti-mouse, Abcam, 1:10000). Western ECL substrate (Biorad; Cat# 1705061) was used to visualize the protein bands using Bio-rad Imaging system (ChemiDoc, Bio-Rad, CA, USA). ImageJ software (NIH, Bethesda, MD, USA) was used for the quantitative analysis. β-actin and GAPDH was used as an internal loading control.

Plasmid construction

Full length of FLAG-tagged KDM3A was amplified from H1299 cDNA by using the following primers. The forward primer: 5'-

CCGGGTACCATGGACTACAAAGACGATGACGACAAGTGCTCACGCTCGGA GAA-3', the reverse primer: 5'-

ccgctcgagtgcctgaagagtttgaacagctgcct-3'. Kpn I and Xho I enzyme digested fragment was purified and ligated into a linearized pcDNA3.1 vector. Positive plasmid was identified by sanger sequencing. Plasmid containing KDM3A shRNA were constructed into pLKO.1 vectors. The target sequencing of KDM3A shRNA was 5'- CTGAAGGTGTGTGTGGAATTT-3'. The sequencing for non-target control was 5'-TCTCGCTTGGGCGAGAGTAAG-3'.

Cell transfection

 5×10^5 cells were seeded into 6-well plates. 12 hours later, siRNA was transfected into cells by using lipofectamine RNAiMAX transfection reagent (Invitrogen; 13778100; USA). The target sequence of KDM3A siRNA1 is

GAAGGCTTCTTAACACCAA. The target sequence of KDM3A siRNA2 is GAAATCAACTACTGTACAA. The non-target siRNA was purchased from Santa Cruz Biotechnology (Cat#: sc-44236, CA, USA). KDM3A overexpression or shRNA plasmid was transfected to cells with Lipo3000 reagent (Invitrogen; L3000075; USA). Transfected cells using empty pcDNA3.1 or pLKO.1 plasmid were used as control. 1%GFP plasmid was co-transfected to cells to visualize the transfection efficiency. KDM3A knockdown stable cell lines were selected by treatment of puromycin (Invivogen, ant-pr-1, CA, USA) at 5 μg/mL for 3 days. Puromycin selected cells were seeded to 10 cm dish for single clone selection. The KDM3A knockdown cell lines were used for the following study.

Wound healing assay

For knocking down or overexpression experiments, 6-well plates were used for cell seeding at a density of 5×10^5 cells after transfection per well. 24 hours later, when the cells had attained around 100% confluence, cells were scraped down the midline of the well using a sterile 200 μ L pipette tip. The cells were then washed with PBS two times, serum-free medium was added, and photographs were taken using Nikon Tie microscope at indicated time points (Nikon Instrument Inc., Ti2-E, Tokyo, Japan). For inhibitor experiments, cells were seeded at a density of 5×10^5 cells per well. 24 hours later, cells were scraped and then washed with PBS two times, serum-free medium contained different inhibitors was added, and photographs were taken at indicated times. The migration distance was analyzed using Image J software (NIH, Bethesda, MD, USA).

Cell proliferation, viability and invasion assays

For the test of cell proliferation, after transfection with siRNA or plasmids for 24 hours, seeds of cells were planted at 1×10^5 cells per well in a 6-well plate, followed by harvesting and quantification using the Cellmeter Spectrum (Nexcellom Bioscience, USA) after 72 hours. For cell viability, 3000 cells were seeded in 96 well plate. 24 hours later, cells were treated with inhibitors for another 72 hours or 24 hours (for cisplatin combination treatment), cell viability was tested using CCK-8 kit (Beyotime, C0038, shanghai, China) and measured by Tecan Spark plate reader (Tecan Trading AG, Switzerland), 5 wells for each group were measured. Using an 8µm hole size, the cell invasion experiment was conducted. Invading chambers were

made of Matrigel (Corning; 354481; USA). For cells transfected with plasmids, at 24 hours post-transfection, cells were separated using 0.25% trypsin-EDTA solution (Coolaber; SL6020-500mL; Beijing, China) and seeded in the upper chamber at 2 × 10⁴ per well. Cell culture medium without FBS were added in the upper chamber, and cell culture medium with FBS were added in the lower chamber. For inhibitor treatment groups, cells were pretreated with inhibitors for 48 hours and then seeded in the upper chamber at 2 × 10⁴ per well, cell culture medium with inhibitors but not FBS were added in the upper chamber, and cell culture medium with both inhibitors and FBS were added in the lower chamber. 20 hours later, upper layer cells were eliminated slightly by a dab of cotton. Cells invaded to the bottom layer were fixed and stained with 1% crystal violet (Beyotime; C0121-100ml; China). Images were captured using a Nikon Ti2-E microscope (Nikon Instrument Inc., Ti2-E, Tokyo, Japan) and cells were counted for 5 views per sample using ImageJ software.

Colony formation experiments

Eight days were spent cultivating NSCLC cells in 6-well plates at a concentration of 500 cells per well. The cells were washed twice with PBS, fixed with 4% paraformaldehyde (Ansiang; L-AX2356; Beijing, China), and then stained using a crystal violet staining solution (Beyotime; C0121-100ml; China). After staining, the cell colonies were photographed by Biorad imaging system (ChemiDoc, Bio-Rad, CA, USA).

Chromatin immunoprecipitation (ChIP)

Chromatin immunoprecipitation (ChIP) was performed according to the instruction of the ChIP Histone H3 [Dimethyl Lys9] Kit (Novus, NBP1-71712). Briefly, cells were crosslinked with 1% formaldehyde for 10 min at room temperature, quenched with 125 mM glycine, and lysed in RIPA lysis buffer. Chromatin was sonicated to an average size of 200 – 1000 bp. After pre-clearing with Protein A/G beads, lysates were incubated overnight at 4°C with an anti-H3K9me2 antibody or IgG control. Immune complexes were captured with Protein A/G beads, washed sequentially with low-salt, high-salt, LiCl, and TE buffers, then eluted in ChIP elution buffer. Crosslinks were reversed at 95°C for 10min, and DNA was purified. Quantitative PCR (qPCR) was performed using SYBR Green Master Mix (Bio-rad, Cat#1725121, USA) on an Applied Biosystems (Carlsbad, CA, USA). Primer sequences using is

listed below: CDH1-forward: 5'-GAACCCTCAGCCAATCAGC-3', reverse: 5'-

CTGACTTCCGCAAGCTCACA-3'. VIM- forward: 5'-

GAGGGGACCCTCTTTCCTAA-3', reverse: 5'-GAGAGTGGCAGAGGACTGGA
-3'. MMP9-forward: 5'-TCACAGGAGCGCCTCCTTAA-3', reverse 5'AGCAAAGCAGCAGCCCAGCA-3'. Enrichment was calculated as % input (2^ (ΔCt [Input-ChIP])) and normalized to IgG controls.

In vivo Xenograft model

The Ningxia Medical University Animal Care and Use Committee authorized the methods used for conducting animal research (KYLL-2024-0794). Nude mice (Gempharmatech Company, 20-22 g, 6-8 weeks of age, female: male = 1:1) were used for xenograft experiments. All animal protocols were performed in the animal facility at Ningxia Medical University in accordance with federal, local, and institutional guidelines. A suspension of 5 × 10⁶ H1299 Cells in RPMI 1640 medium were injected into nude mice subcutaneously. The volume and body weight of the mice was recorded, and tumor volumes were measured and calculated [0.5 × L (long dimension) × W² (short dimension)] twice a week. The mice were sacrificed by CO₂ inhalation around three weeks after the injection. The tumors were removed, weighted and retained for hematoxylin-eosin (HE) staining and immunohistochemistry (IHC) staining.

Ethic and clinical sample collection

A total of 30 lung adenocarcinoma patients who underwent surgical resection between 2023-2024 without chemotherapy or radiation therapy were included, patients' clinical characteristics and tumor and adjacent tumor samples were collected.

Hematoxylin-eosin (HE) and immunohistochemistry (IHC) staining

Tumor tissues were fixed in formalin solution immediately after harvesting. Tissues were dehydrated with ethanol, embedded with paraffin, and sectioned into slides, for the staining procedure. HE staining were performed following the guidance of HE stains solution kit (Applygen, C1410, Beijing, China). Briefly, slides were deparaffinize and rehydrate by emerging in Xylene, 100% ethanol, 95% ethanol, 80% ethanol for 5min each. Then the slides were put into deionized H₂O for 3 times, 3 min each time. The deparaffinized slides were stained with hematoxalin for 3 minutes.

And washed with deionized H₂O. Then the slides were washed with Ethanol hydrochloride and deionized H₂O. Lastly, the slides were stained by eosin for 2min and washed with deionized H₂O. IHC staining were performed following the protocol provided by Elabscience (Cat#: E-IR-R220, Wuhan, China). Briefly, slides were performed dewaxing and antigen-retrieval using Dewaxing/Antigen Retrieval Buffer provided in the kit in a pressure cooker for 20 min. Dry the liquid and incubate with SP reagent B at room temperature for 15min. After washed with TBS for 2min × 3 times, the slides were stained with primary antibodies (KDM3A (1:100), H3K9me2 (4658T, 1:200), Ki67 (Cell Signaling Technology, 9129T, 1:500,USA), CD 34 (Abcam, ab81289, 1:200,USA), FOXP3 (Abcam, ab20034, 1:500,USA) at 4°C overnight. Washed with TBS for 3 times and then stained with HRP-labeled secondary antibody for 1 hour at RT. Lastly, positive signals were visualized by adding the DAB buffer provided in the Kit. All the slides were dehydrated by 85% ethanol, 95% ethanol \times 2, absolute ethanol \times 2, 3min each. The slides were transparentized with xylene and sealed with neutral gum. The Zeiss Axio Imager M2 microscope was used to image the slides. (Carl Zeiss, Oberkochen, Germany). For clinical slides, KDM3A, H3K9me2 and FOXP3 IHC staining was scored by pathologist as 0 (no positive staining), 1+ (< 15%), 2+ (15-30%), and 3+ (> 30%) of the cells stained positive). Spearman correlation was employed to evaluate the correlation between the three protein's expression.

Ethical statement

This study was approved by the Research Ethics Committee of Ningxia Medical University, authorized the methods used for conducting animal research and patient samples collection with informed consent (Approved number: KYLL-2024-0794).

Statistical analysis

Images were analyzed by Image J software. GraphPad Prism 8.02 (GraphPad, La Jolla, CA, USA) accustomed to analyzing the data. Three separate experiments' results are shown as mean ± standard deviation (SD). SD was calculated by calculating the squared difference of each data point from the mean, summing these squared differences to get the variance, and then taking the square root of the variance. Student t-test was employed in the evaluation between groups. Spearman correlation

analysis was employed to evaluate the correlation between protein expression of clinical samples. p < 0.05 was considered in the statistical sense.

Data availability

The original data for statistically analysis were supplemented in the "original data.xls" file which contains per mouse body weight and tumor measure tables.

RESULTS

Knockdown of KDM3A inhibited cell proliferation and migration

KDM3A facilitates the enzymatic removal of methyl groups from transcriptionally repressive histone H3 lysine 9 mono- and dimethylation marks (H3K9me1/me2), exhibiting a substrate preference for dimethylated residues, thereby modulating transcriptional regulation [25]. To investigate the functional impact of KDM3A on NSCLC, we knocked down its expressing using siRNAs (Figure 1A). Subsequent evaluation of cell proliferation in three cancer cell lines (H1299, A549 and HCC827) revealed that KDM3A sianigicantly diminished proliferation in all the cell lines compared to the control group (Figure 1B). Furthermore, the wound-healing assay demonstrated a significant reduction in cancer cell migration (Figure 1C) following KDM3A knockdown in H1299, A549 and HCC827 cell lines (Figure 1D). These preliminary results indicate that KDM3A knockdown hinders both tumor cell proliferation and migration in NSCLC.

Knockdown of KDM3A increased H3K9me2 and inhibited EMT-related signaling

To explore the mechanism by which KDM3A regulates migration in NSCLC. We evaluated metastasis-related proteins by western blot. As shown in Figure 2A (upper panel and lower panel), KDM3A knockdown significantly increased H3K9me2 levels in both siRNA groups (si1 and si2) compared to the control group (Ctrl siR) across H1299, A549 and HCC827 cell lines, without affecting KDM3B expression. E-cadherin protein level increased, while MMP-9 and Vimentin decreased in the KDM3A knockdown groups (si1 and si2) compared to the control group (Ctrl siR). In contrast, both the expression of FAK, phosphor-FAK (Tyr397) and the pFAK/FAK ratio remained unchanged (Figure 2B). Quantification confirmed a significant increase in E-cadherin and H3K9me2, significant decresed in MMP-9 and Vimentin

upon KDM3A knockdown), while no significant change in pFAK, FAK or pFAK/FAK ratio (Figure 2B, lower and right panel). We next used qRT-PCR to assess the mRNA expression of EMT related genes and other KDMs. Mirroring the protein data, CDH1 (E-cadherin) mRNA significantly upregulated in the si1 and si2 groups, while the mRNA expression of VIM and MMP-9 decreased. However, no significant differences were observed in the mRNA expression of KDM3B or KDM3C (Figure 2C). Colletively, these results demonstrate that KDM3A knockdown upregulates H3K9me2 and suppresses the expression of key genes (VIM, MMP-9) associated with cell invasion. This indicates that KDM3A promotes tumor cell invasion in an H3K9me2-dependent manner.

Overexpression of KDM3A decreased H3K9me2 and promoted EMT-related signaling

Following the confirmation that KDM3A knockdown impedes the growth and invasion of NSCLC cells, we investigated the functional consequences of KDM3A overexpression. We overexpressed KDM3A in H1299, A549 and HCC827 cell lines and analyzed key markers by western blotting. KDM3A overexpression significantly decreased H3K9me2 levels across all the three cell lines without altering KDM3B expression, compared to the control group (Figure 3A, left panel and right panel). Besides, KDM3A overexpression led to a substantial reduction in E-cadherin expression and an elevation in Vimentin and MMP-9 expression, at both mRNA level (Figure 3B) and protein level (Figure 3C).

To elucidate the direct regulatory mechanism of KDM3A on the EMT-related genes, we performed ChIP qPCR using H3K9me2 antibody. In control cells, we observed significant enrichment of the repressive H3K9me2 mark at the promoter regions of VIM and MMP9 (Figure 4A, left panel). Importantly, KDM3A overexpression significantly reduced H3K9me2 occupancy at these promoters (Figure 4A, right panel), indicating direct epigenetic de-repression. In contrast, no significant H3K9me2 enrichment was detected at the CDH1 (E-cadherin) promoter under either condition (Figure 4A), suggesting an alternative regulatory mechanism. Since previous studies have indicated that KDM3A can activate the STAT3 pathway, which suppresses E-cadherin expression [22-25], we investigated this possibility. We found that KDM3A knockdown inhibited STAT3 and p-STAT3 (Y705) expression, whereas KDM3A overexpression enhanced their levels. In summary, these results

demonstrate that KDM3A promotes EMT and invasion through distinct mechanisms: it directly reduces H3K9me2 at the VIM and MMP9 promoters to activate their expression, while it likely suppresses E-cadherin indirectly by activating the STAT3 pathway.

KDM3A overexpression promoted cell proliferation, migration and invasion

To further characterize the pro-tumorigenic role of KDM3A, we assessed its impact on proliferation, clonogenicity, migration, and invasion. Cell counting assays revealed that KDM3A overexpression significantly enhanced the proliferation of H1299, A549 and HCC827 cell lines (Figure 5A). Consistent with this, a colony formation assay demonstrated that KDM3A overexpression increased the colony formation ability of all the three cell lines, compared to the control group (Figure 5B). Additionally, a 36-hour wound healing assay revealed enhanced migration of cancer cells following KDM3A overexpression (Figure 5C, upper panel and Figure 5D, left panel). The trans-well experiment also indicated increased invasive activity of cancer cells upon KDM3A overexpression (Figure 5C, lower panel and Figure 5D, right panel). These findings demonstrate that KDM3A overexpression drives NSCLC progression by enhancing key cancer hallmarks, including proliferation, clonogenicity, migration, and invasion.

Knockdown of KDM3A decreased tumor formation in vivo

To investigate the role of KDM3A in tumor growth *in vivo*, we established stable KDM3A shRNA knockdown H1299 cell lines using shRNA. As confirmed by western blot, KDM3A was stably knockdown in the shKDM3A group compared to the shCtrl group (Figure 6A left panel and right panel). The body weights of the mice showed no significant difference between the shCtrl and shKDM3A group (Figure 6B), indicating that KDM3A knockdown did not cause systemic toxicity. However, tumor growth was significantly inhibited upon KDM3A knockdown, as evidenced by reduced tumor volume and tumor weight compared to the shCtrl group (Figure 6C-E).

Furthermore, IHC analysis of the xeograft tumor revealed that the shKDM3A group had decreased KDM3A expression, increased H3K9me2 levels, reduced expression of proliferation marker Ki-67 and the angiogenesis marker CD34 (Figure 6F). These results indicate that KDM3A knockdown suppresses tumor cell proliferation and angiogenesis *in vivo*. Taken together, these *in vivo* findings demonstrate that KDM3A

knockdown significantly inhibits tumor growth, consistent with our *in vitro* observation.

KDM3A is a potential therapeutic target for NSCLC

To evaluate the therapeutic potential of targeting KDM3A in NSCLC, we treated H1299, A549, and HCC827 cell lines with two KDM3A inhibitors with limited selectivity, CBA-1 and IOX-1. Both compounds significantly reduced cell viability (Figures 7A and 7B) and potently suppressed migration and invasion in H1299 cells (Figure 7C). Surprisingly, when treating the cells with the two inhibitors in combination with cisplatin, no synergetic effect was observed (Figure S1 A-D). In 30 primary NSCLC specimens, we stained for the expression of KDM3A, H3K9me2 and FOXP3 (Figure 7D) and assessed the relationship between KDM3A, H3K9me2, FOXP3+ Treg infiltration, and TNM stage. KDM3A expression exhibited a significant inverse correlation with H3K9me2 levels (r = -0.4635, p < 0.01; Figure 7E), consistent with its demethylase activity. Strikingly, KDM3A positively correlated with FOXP3 expression (r = 0.5158, p < 0.0001; Figure 7F), suggesting a potential role in Treg recruitment or expansion. Furthermore, elevated KDM3A was associated with metastasis (M stage) (r = 0.4285, p = 0.0182), supporting its prometastatic function. Collectively, these findings indicated that pharmacological inhibition of KDM3A suppresses tumor growth and invasive potential, whereas its overexpression in clinical specimens was associated with metastatic progression and infiltration of immunosuppressive regulatory T cells.

DISCUSSION

This study comprehensively investigated the role of the H3K9me2 demethylase KDM3A in NSCLC progression. We demonstrated that KDM3A is a key epigenetic driver of epithelial-mesenchymal transition (EMT) and metastasis. KDM3A knockdown increased global H3K9me2 levels, which led to the upregulation of the epithelial marker E-cadherin and the downregulation of the mesenchymal markers Vimentin and MMP-9, thereby suppressing cell proliferation, migration, and invasion. Conversely, KDM3A overexpression reduced H3K9me2 levels, promoted a mesenchymal phenotype, and enhanced aggressive cellular behaviors. These in vitro findings were corroborated in vivo, where KDM3A knockdown significantly inhibited tumor growth in xenograft models. Mechanistically, we found that KDM3A directly

reduced H3K9me2 occupancy at the promoters of VIM and MMP9, activating their transcription. In parallel, KDM3A downregulated E-cadherin expression by activating the STAT3 signaling pathway. Clinically, elevated KDM3A expression in NSCLC patient samples was inversely correlated with H3K9me2 levels and positively associated with metastasis and FOXP3+ Treg infiltration, underscoring its clinical relevance.

As cancer advances, cells known as epithelial tumors may undergo EMT, thereby profoundly altering the characteristics of the tumor cells. This caused the disappearance of epithelial markers (i.e., E-cadherin), alterations in cell polarity and intercellular junctions, and a rise in mesenchymal indicators (i.e., Vimentin) [26]. Thus, with increasing disease severity, the expression of E-cadherin tends to decrease, while the expression of Vimentin tends to increase and can be used as a marker.

In this study, KDM3A knockdown increased H3K9me2 levels, elevated expression of E-cadherin, and decreased expression of Vimentin and MMP-9. Subsequent analysis indicated that the knockdown and inhibition of KDM3A inhibited tumor cell proliferation, migration and invasion. Conversely, KDM3A overexpression decreased H3K9me2 levels, reduced E-cadherin expression, and increased Vimentin and MMP-9 expression. Experiments conducted in KDM3A overexpression cells showed a notable increase in tumor cell invasion, migration, and proliferation. Mice xenograft model revealed that knockdown of KDM3A reduced tumor growth *in vivo*. KDM3A was found to be correlated with H3K9me2, metastasis stage and Treg infiltration in patient samples.

Thus, our results implied that the control of invasion-related genes by the H3K9 methylation regulator KDM3A influences the proliferation, migration, and invasion of NSCLC. The evidence strongly supports KDM3A's role in promoting NSCLC cell proliferation and invasion via H3K9 demethylation of VIM and MMP-9 and regulation of E-cadherin. Thus, KDM3A is important in regulating EMT in non-small cell lung cancers.

In addition to having an epigenetic landscape effect on H3K9me2, KDM3A also has other epigenetic effects. KDM3A stimulated FOXP3 transcription by directly attaching to the FOXP3 promoter, which in turn induced the release of downstream inhibitory cytokines (TGF-β1, IL-35, and HO-1) linked with FOXP3, ultimately

promoting immune escape from lung adenocarcinoma [27]. In our study, we also found a significant positive correlation between KDM3A and FOXP3 expression in clinical NSCLC patient samples, leading us to further explore the role of KDM3A in immune infiltration of NSCLC in the future. KDM3A regulated epidermal growth factor receptor (EGFR) expression through kruppel-like factor 5 (KLF5) and SMAD family member 4 (SMAD4) [28]. Let-7d, KDM3A, and ENO2 form an epigenetic network in the pathogenesis of preeclampsia and let-7d acts as a miRNA that inhibits the development of preeclampsia through the down-regulation of KDM3A expression and the promotion of ENO2 methylation, thereby inhibiting trophoblast development and inducing apoptosis, thus promoting the progression of PE [29].

According to the research, histone methylation status is associated with cell proliferation, survival, differentiation, and gene expression in human diseases [30, 31]. Several lysine methyltransferases (KMTs) coordinate the methylation of lysine residues; most of these methylations are reversible and mediated by lysine-specific demethylases (KDMs) [32]. Understanding the genesis of cancer requires unraveling the dysregulated regulators of histone lysine methylation and exploring their underlying processes. Our systematic examination of the H3K9 regulator, KDM3A, in NSCLC, revealed that it promotes cell proliferation and invasion by demethylating H3K9me2 of VIM and MMP-9. Consistent with our results, it has been reported that aberrant H3K9 methylation leads to the transcriptional repression of various tumor suppressor genes and related genes in cancer cells [33], consequently influencing the capacity of cancer cells to multiply, spread and infiltrate, as seen in malignant colorectal cancer [34], melanoma [35], prostate cancer [36], gastric cancer [37], breast cancer [38], lung adenocarcinoma [39], and triple-negative breast cancer [40]. Aberrant H3K9 methylation was linked to cells' proliferation, migration, and invasive capability in these tumors. Besides, KDM3A was identified to demethylate H3K9me2 at the promoter of specificity protein 1 (SP1) and to increase SP1 transcription in osteosarcoma and pancreatic cancer in a study by Wang et al. Restoring SP1 prevented cancer cells from proliferating and spreading and restored glycolytic flow to cells suppressed by KDM3A knockdown. As a result, KDM3A knockdown dramatically reduced the development of tumors in vivo and in vitro and inhibited the aerobic glycolysis of cancer cells [41, 42].

Additionally, KDM3A has been linked with promoting invasion and migration in NSCLC [43]. Moreover, KDM3A overexpression was identified in colorectal cancer specimens, and KDM3A knockdown reduced MMP-9 expression and enzyme activity. This knockdown inhibited colorectal cancer cell migration, invasion, and metastasis [44]. MMP-9 belongs to the MMP family and is a zinc-dependent peptidase expressed by many cellular [45]. E-cadherin inhibits cell migration and dissemination by mediating cell-cell adhesion dependent homologous interactions via Ca²⁺ [21]. Matrix metalloproteinases (MMPs) are zinc-dependent proteases with specific protein hydrolysis effects. MMP-9-mediated collagen degradation promoted cancer cell invasion and metastasis [46, 47]. The downregulation of E-cadherin diminished cellcell adhesion, fostering cell viability and β-catenin activation, thus promoting malignancy [48]. Our study similarly demonstrated that in the three lung cancer cell lines, KDM3A knockdown reduced the expression of cell invasion-related genes like Vimentin and MMP-9, while increasing the expression of E-cadherin, ultimately inhibiting cancer cell migration. Conversely, KDM3A overexpression promoted cell migration, invasion and colony formation, as well as the expression of EMT genes in NSCLC cells.

There are a number of previous studies on the effects of KDM3A on lung cancer, but detailed studies on the epigenetic effects and specific downstream targets of KDM3A and H3K9me2 on lung cancer are still lacking. We comprehensively explored and elaborated the changes in H3K9me2 levels after KDM3A overexpression and knockdown and their effects on NSCLC cell invasion. Using ChIP qPCR, we identified the H3K9me2 occupancy at promoter of VIM and MMP-9 was directly modulated by KDM3A, with knockdown increasing and overexpression decreasing occupancy, thus regulating VIM and MMP-9 expression. KDM3A downregulated Ecadherin expression via the p-STAT3 signaling pathway. Together with previous published research [23], we concluded that KDM3A indirectly regulated CDH1 expression might through STAT3 signaling pathway. Using both in vitro and in vivo experiments, along with clinical samples, strengthens the persuasiveness of the findings. In vivo experiments offer several advantages, such as precise control of exposure conditions, simultaneous measurement of multiple effects, assessment of host characteristics, and evaluation of mechanisms. Animal models have become indispensable tools for investigating cancer mechanisms. Numerous experiments have explored how KDM3A influences NSCLC by employing *in vivo* experiments for validation. One study reported that in tests with nude mice, microRNA-449a targeted the KDM3A/ hypoxia-inducible factor (HIF-1α) axis to suppress the advancement of lung cancer [49]. Furthermore, researchers have shown that KDM3A expression influenced the substantial decrease of EGFR in NSCLC with EGFR mutations. In this study, we used three cell lines with RAS mutation or EGFR mutation. All the three cell lines showed significant migratory and invasive response upon KDM3A modulation, indicating the KDM3A signaling pathway in NSCLC is independent of genetic background of the cancer cells.

Lung cancer progression is regulated by multiple mechanisms mediated by key regulators. Additionally, the anticancer impact of the inhibitor BIX was attributed to the downregulation of phosphorylated BCKD Elalpha subunit (BCKDHA) by KDM3A [1]. Authors xenografted H1299 cells into nude mice and examined the result of the long-chain non-coding RNA small nucleolar RNA host gene 4 (SNHG4) on NSCLC. The experiments concluded that KDM3A inhibits p21, and RNA SNHG4 contributes to the oncogenic effect of NSCLC progression through the regulation of KDM3A, aligning with our findings [43]. In this study, we conducted animal experiments by introducing KDM3A shRNA into cells, then transplanting the KDM3A stable knockdown cells into mice. We investigated the impact of KDM3A knockdown on tumor growth by comparing tumor volume and weight between the knockdown group and control group. The acquired experimental data demonstrated that tumor weight and tumor volume in the KDM3A knockdown group were substantially lower than those in the control group. This outcome, together with our previous in vitro experiments, proves that KDM3A knockdown significantly inhibited tumor growth in both in vitro and in vivo.

In studies targeting NSCLC, abnormally elevated KDM3A expression has been demonstrated in cancerous tissues, and KDM3A knockdown has been shown to inhibit key cancer cell functions, highlighting its high clinical potential [50]. However, while KDM inhibitors are in development, the compounds reported so far lack selectivity for the KDM3 subfamily or its specific isoforms. This largely because most of the KDM3 crystal structures remain undetermined, and existing inhibitors often target the catalytic mechanisms common to a wide range of KDM [51]. In this study, we used two KDM3A inhibitors with limited selectivity, CBA-1 and IOX-1,

and found that treatment significantly inhibited cell viability, migratory and invasive ability of NSCLC cells. However, we acknowledge important limitations: currently available KDM3A inhibitors lack sufficient specificity. CBA-1 has additional anti-Wnt activity [52], while IOX-1 broadly targets multiple KDMs [51]. These off-target effects may confound the interpretation of KDM3A's specific function in our models. The development of more potent and highly specific KDM3A inhibitors will be crucial for future therapeutic studies.

This study reveals the critical role of KDM3A in promoting non-small cell lung cancer (NSCLC) cell proliferation and invasion through H3K9 demethylation. Clinical sample analysis further linked high KDM3A expression to metastasis and immune infiltration. These results demonstrate KDM3A's consistent role in NSCLC progression across experimental and clinical settings, supporting its potential as both a prognostic marker and therapeutic target. Targeting KDM3A may contribute to precision medicine approaches and open new avenues for the epigenetic treatment of NSCLC.

This study has several limitations. First, while we identified that KDM3A downregulates H3K9me2 in NSCLC, we did not thoroughly investigate whether its knockdown or overexpression influences activity of other KDMs. Second, we found that KDM3A regulates VIM (vimentin) and MMP-9 through removing promoter occupancy of H3K9me2. Unfortunately, we could not find a ChIP grade antibody for KDM3A and could not get the KDM3A occupancy data in the EMT genes. Through literature consultation and preliminary experiments, we speculated KDM3A regulated CDH1 through STAT3 signaling pathway, this need to be further validated by rescue experiment. Third, since KDM3A expression induces a global change in H3K9me2 levels, its potential regulation of tumor suppressor genes needs to be verified in subsequent studies. Fourth, regarding the correlation between KDM3A and immune infiltration, we only observed this association in patient tissues. Although previous studies have shown that KDM3A regulates FOXP3 transcription in lung cancer [27], further validation in immunocompetent mouse model is necessary to definitively investigate the role of KDM3A in immune infiltration.

Although our evidence indicates a direct association between KDM3A and genes controlling cell invasion, more in-depth studies are required to elucidate the

regulatory mechanisms. A comprehensive understanding of the epigenetic regulation

mediated by KDM3A is crucial and may involve coordinated interactions between

histone modifications and possibly nucleosome structure.

CONCLUSION

In conclusion, our study establishes KDM3A as a key epigenetic driver of NSCLC

progression, where it promotes tumor growth and invasion through the regulation of

H3K9 methylation. This work positions KDM3A as a compelling therapeutic target

for the development of novel treatment strategies against NSCLC.

ACKNOWLEDGMENTS

We acknowledge the generous support of program of Ningxia Medical University

(XM2021004). The authors thank pathology department of General Hospital of

Ningxia Medical University for their support on IHC staining.

Conflicts of interest: Authors declare no conflicts of interest.

Funding: This project is supported by program of Ningxia Medical University

(XM2021004).

Submitted: September 4, 2024

Accepted: October 12, 2025

Published online: November 3, 2025

20

REFERENCES

- [1] Kim JH, Kim J, Im SS, Lee JH, Hwang S, Chang EJ, et al. BIX01294 inhibits EGFR signaling in EGFR-mutant lung adenocarcinoma cells through a BCKDHA-mediated reduction in the EGFR level. Exp Mol Med. 2021;53(12):1877-87.
- [2] Mo WL, Deng LJ, Cheng Y, Yu WJ, Yang YH, Gu WD. Circular RNA hsa_circ_0072309 promotes tumorigenesis and invasion by regulating the miR-607/FTO axis in non-small cell lung carcinoma. Aging (Albany NY). 2021;13(8):11629-45.
- [3] Chen B, Wang J, Wang J, Wang H, Gu X, Tang L, et al. A regulatory circuitry comprising TP53, miR-29 family, and SETDB1 in non-small cell lung cancer. Biosci Rep. 2018;38(5).
- [4] Heller G, Altenberger C, Steiner I, Topakian T, Ziegler B, Tomasich E, et al. DNA methylation of microRNA-coding genes in non-small-cell lung cancer patients. J Pathol. 2018;245(4):387-98.
- [5] Souza BK, Freire NH, Jaeger M, de Farias CB, Brunetto AL, Brunetto AT, et al. EHMT2/G9a as an Epigenetic Target in Pediatric and Adult Brain Tumors. Int J Mol Sci. 2021;22(20).
- [6] Wang Z, Chen J, Gao C, Xiao Q, Wang XW, Tang SB, et al. Epigenetic Dysregulation Induces Translocation of Histone H3 into Cytoplasm. Adv Sci (Weinh). 2021;8(19):e2100779.
- [7] Hansen AM, Ge Y, Schuster MB, Pundhir S, Jakobsen JS, Kalvisa A, et al. H3K9 dimethylation safeguards cancer cells against activation of the interferon pathway. Sci Adv. 2022;8(11):eabf8627.
- [8] Hou X, Li Q, Yang L, Yang Z, He J, Li Q, et al. KDM1A and KDM3A promote tumor growth by upregulating cell cycle-associated genes in pancreatic cancer. Exp Biol Med (Maywood). 2021;246(17):1869-83.
- [9] Ma Y, Nenkov M, Schröder DC, Abubrig M, Gassler N, Chen Y. Fibulin 2 Is Hypermethylated and Suppresses Tumor Cell Proliferation through Inhibition of Cell Adhesion and Extracellular Matrix Genes in Non-Small Cell Lung Cancer. Int J Mol Sci. 2021;22(21).
- [10] Li R, Ong SL, Tran LM, Jing Z, Liu B, Park SJ, et al. Chronic IL-1β-induced inflammation regulates epithelial-to-mesenchymal transition memory phenotypes via epigenetic modifications in non-small cell lung cancer. Sci Rep. 2020;10(1):377.

- [11] Montavon T, Shukeir N, Erikson G, Engist B, Onishi-Seebacher M, Ryan D, et al. Complete loss of H3K9 methylation dissolves mouse heterochromatin organization. Nat Commun. 2021;12(1):4359.
- [12] Monaghan L, Massett ME, Bunschoten RP, Hoose A, Pirvan PA, Liskamp RMJ, et al. The Emerging Role of H3K9me3 as a Potential Therapeutic Target in Acute Myeloid Leukemia. Front Oncol. 2019;9:705.
- [13] Soini Y, Kosma VM, Pirinen R. KDM4A, KDM4B and KDM4C in non-small cell lung cancer. Int J Clin Exp Pathol. 2015;8(10):12922-8.
- [14] Zhang B, Zhang J, Liu G, Guo X, Liu X, Chen J. KDM3A Inhibition Ameliorates Hyperglycemia-Mediated Myocardial Injury by Epigenetic Modulation of Nuclear Factor Kappa-B/P65. Front Cardiovasc Med. 2022;9:870999.
- [15] Zhang H, Wang Y, Bian X, Yin H. MicroRNA-194 acts as a suppressor during abdominal aortic aneurysm via inhibition of KDM3A-mediated BNIP3. Life Sci. 2021;277:119309.
- [16] Padeken J, Methot SP, Gasser SM. Establishment of H3K9-methylated heterochromatin and its functions in tissue differentiation and maintenance. Nat Rev Mol Cell Biol. 2022;23(9):623-40.
- [17] Shait Mohammed MR, Zamzami M, Choudhry H, Ahmed F, Ateeq B, Khan MI. The Histone H3K27me3 Demethylases KDM6A/B Resist Anoikis and Transcriptionally Regulate Stemness-Related Genes. Front Cell Dev Biol. 2022;10:780176.
- [18] Fang W, Liao C, Shi R, Simon JM, Ptacek TS, Zurlo G, et al. ZHX2 promotes HIF1α oncogenic signaling in triple-negative breast cancer. Elife. 2021;10.
- [19] Zhang W, Liu R, Zhang L, Wang C, Dong Z, Feng J, et al. Downregulation of miR-335 exhibited an oncogenic effect via promoting KDM3A/YAP1 networks in clear cell renal cell carcinoma. Cancer Gene Ther. 2022;29(5):573-84.
- [20] Zhao G, Yu H, Ding L, Wang W, Wang H, Hu Y, et al. microRNA-27a-3p delivered by extracellular vesicles from glioblastoma cells induces M2 macrophage polarization via the EZH1/KDM3A/CTGF axis. Cell Death Discov. 2022;8(1):260.
- [21] Lee Y, Ko D, Yoon J, Lee Y, Kim S. TMEM52B suppression promotes cancer cell survival and invasion through modulating E-cadherin stability and EGFR activity. J Exp Clin Cancer Res. 2021;40(1):58.
- [22] Zhang B, Liu G, Huang B, Liu H, Jiang H, Hu Z, et al. KDM3A Attenuates Myocardial Ischemic and Reperfusion Injury by Ameliorating Cardiac Microvascular

Endothelial Cell Pyroptosis. Oxid Med Cell Longev. 2022;2022:4622520.

- [23] Kim H, Kim D, Choi SA, Kim CR, Oh SK, Pyo KE, et al. KDM3A histone demethylase functions as an essential factor for activation of JAK2-STAT3 signaling pathway. Proc Natl Acad Sci U S A. 2018;115(46):11766-71.
- [24] Zhang BF, Jiang H, Chen J, Guo X, Hu Q, Yang S. KDM3A inhibition attenuates high concentration insulin-induced vascular smooth muscle cell injury by suppressing MAPK/NF-κB pathways. Int J Mol Med. 2018;41(3):1265-74.
- [25] Xiong H, Hong J, Du W, Lin YW, Ren LL, Wang YC, et al. Roles of STAT3 and ZEB1 proteins in E-cadherin down-regulation and human colorectal cancer epithelial-mesenchymal transition. J Biol Chem. 2012;287(8):5819-32.
- [26] Paolillo M, Schinelli S. Extracellular Matrix Alterations in Metastatic Processes. Int J Mol Sci. 2019;20(19).
- [27] Li Y, Yang W, Wu B, Liu Y, Li D, Guo Y, et al. KDM3A promotes inhibitory cytokines secretion by participating in TLR4 regulation of Foxp3 transcription in lung adenocarcinoma cells. Oncol Lett. 2017;13(5):3529-37.
- [28] Li J, Yuan S, Norgard RJ, Yan F, Sun YH, Kim IK, et al. Epigenetic and Transcriptional Control of the Epidermal Growth Factor Receptor Regulates the Tumor Immune Microenvironment in Pancreatic Cancer. Cancer Discov. 2021;11(3):736-53.
- [29] Xu Q, Song Y, Lu L. Overexpression of let-7d explains down-regulated KDM3A and ENO2 in the pathogenesis of preeclampsia. J Cell Mol Med. 2021;25(17):8127-39.
- [30] Zhang X, Wang X, Wu T, Yin W, Yan J, Sun Y, et al. Therapeutic potential of targeting LSD1/ KDM1A in cancers. Pharmacol Res. 2022;175:105958.
- [31] Wang Z, Cai H, Zhao E, Cui H. The Diverse Roles of Histone Demethylase KDM4B in Normal and Cancer Development and Progression. Front Cell Dev Biol. 2021;9:790129.
- [32] Shi Y, Lan F, Matson C, Mulligan P, Whetstine JR, Cole PA, et al. Histone demethylation mediated by the nuclear amine oxidase homolog LSD1. Cell. 2004;119(7):941-53.
- [33] Yuan L, Sun B, Xu L, Chen L, Ou W. The Updating of Biological Functions of Methyltransferase SETDB1 and Its Relevance in Lung Cancer and Mesothelioma. Int J Mol Sci. 2021;22(14).
- [34] Chen B, Zhu Y, Chen J, Feng Y, Xu Y. Activation of TC10-Like Transcription

- by Lysine Demethylase KDM4B in Colorectal Cancer Cells. Front Cell Dev Biol. 2021;9:617549.
- [35] Zhang SM, Cai WL, Liu X, Thakral D, Luo J, Chan LH, et al. KDM5B promotes immune evasion by recruiting SETDB1 to silence retroelements. Nature. 2021;598(7882):682-7.
- [36] Baratchian M, Tiwari R, Khalighi S, Chakravarthy A, Yuan W, Berk M, et al. H3K9 methylation drives resistance to androgen receptor-antagonist therapy in prostate cancer. Proc Natl Acad Sci U S A. 2022;119(21):e2114324119.
- [37] Wang L, Chen J, Zuo Q, Wu C, Yu T, Zheng P, et al. Calreticulin enhances gastric cancer metastasis by dimethylating H3K9 in the E-cadherin promoter region mediating by G9a. Oncogenesis. 2022;11(1):29.
- [38] Zhang Z, Chen B, Zhu Y, Zhang T, Zhang X, Yuan Y, et al. The Jumonji Domain-Containing Histone Demethylase Homolog 1D/lysine Demethylase 7A (JHDM1D/KDM7A) Is an Epigenetic Activator of RHOJ Transcription in Breast Cancer Cells. Front Cell Dev Biol. 2021;9:664375.
- [39] Jin X, Zhang B, Zhang H, Yu H. Smoking-associated upregulation of CBX3 suppresses ARHGAP24 expression to activate Rac1 signaling and promote tumor progression in lung adenocarcinoma. Oncogene. 2022;41(4):538-49.
- [40] Xu P, Xiong W, Lin Y, Fan L, Pan H, Li Y. Histone deacetylase 2 knockout suppresses immune escape of triple-negative breast cancer cells via downregulating PD-L1 expression. Cell Death Dis. 2021;12(8):779.
- [41] Chopra A, Willmore WG, Biggar KK. Insights into a Cancer-Target Demethylase: Substrate Prediction through Systematic Specificity Analysis for KDM3A. Biomolecules. 2022;12(5).
- [42] Xu Y, Huang Z, Yu X, Chen K, Fan Y. Integrated genomic and DNA methylation analysis of patients with advanced non-small cell lung cancer with brain metastases. Mol Brain. 2021;14(1):176.
- [43] Wang F, Quan Q. The long non-coding RNA SNHG4/microRNA-let-7e/KDM3A/p21 pathway is involved in the development of non-small cell lung cancer. Mol Ther Oncolytics. 2021;20:634-45.
- [44] Peng K, Su G, Ji J, Yang X, Miao M, Mo P, et al. Histone demethylase JMJD1A promotes colorectal cancer growth and metastasis by enhancing Wnt/β-catenin signaling. J Biol Chem. 2018;293(27):10606-19.
- [45] Zamanian M, Hajizadeh M, Shamsizadeh A, Moemenzadeh M, Amirteimouri

- M, Elshiekh M, et al. Effects of naringin on physical fatigue and serum MMP-9 concentration in female rats. Pharm Biol. 2017;55(1):423-7.
- [46] Geng X, Chen C, Huang Y, Hou J. The prognostic value and potential mechanism of Matrix Metalloproteinases among Prostate Cancer. Int J Med Sci. 2020;17(11):1550-60.
- [47] Al-Sadi R, Engers J, Haque M, King S, Al-Omari D, Ma TY. Matrix Metalloproteinase-9 (MMP-9) induced disruption of intestinal epithelial tight junction barrier is mediated by NF-κB activation. PLoS One. 2021;16(4):e0249544.
- [48] Pence LJ, Kourtidis A, Feathers RW, Haddad MT, Sotiriou S, Decker PA, et al. PLEKHA7, an Apical Adherens Junction Protein, Suppresses Inflammatory Breast Cancer in the Context of High E-Cadherin and p120-Catenin Expression. Int J Mol Sci. 2021;22(3).
- [49] Hu S, Cao P, Kong K, Han P, Deng Y, Li F, et al. MicroRNA-449a delays lung cancer development through inhibiting KDM3A/HIF-1α axis. J Transl Med. 2021;19(1):224.
- [50] Zhan M, Wen F, Liu L, Chen Z, Wei H, Zhou H. JMJD1A promotes tumorigenesis and forms a feedback loop with EZH2/let-7c in NSCLC cells. Tumour Biol. 2016;37(8):11237-47.
- [51] Yoo J, Jeon YH, Cho HY, Lee SW, Kim GW, Lee DH, et al. Advances in Histone Demethylase KDM3A as a Cancer Therapeutic Target. Cancers (Basel). 2020;12(5).
- [52] Zhang W, Sviripa VM, Xie Y, Yu T, Haney MG, Blackburn JS, et al. Epigenetic Regulation of Wnt Signaling by Carboxamide-Substituted Benzhydryl Amines that Function as Histone Demethylase Inhibitors. iScience. 2020;23(12):101795.

FIGURES WITH LEGENDS

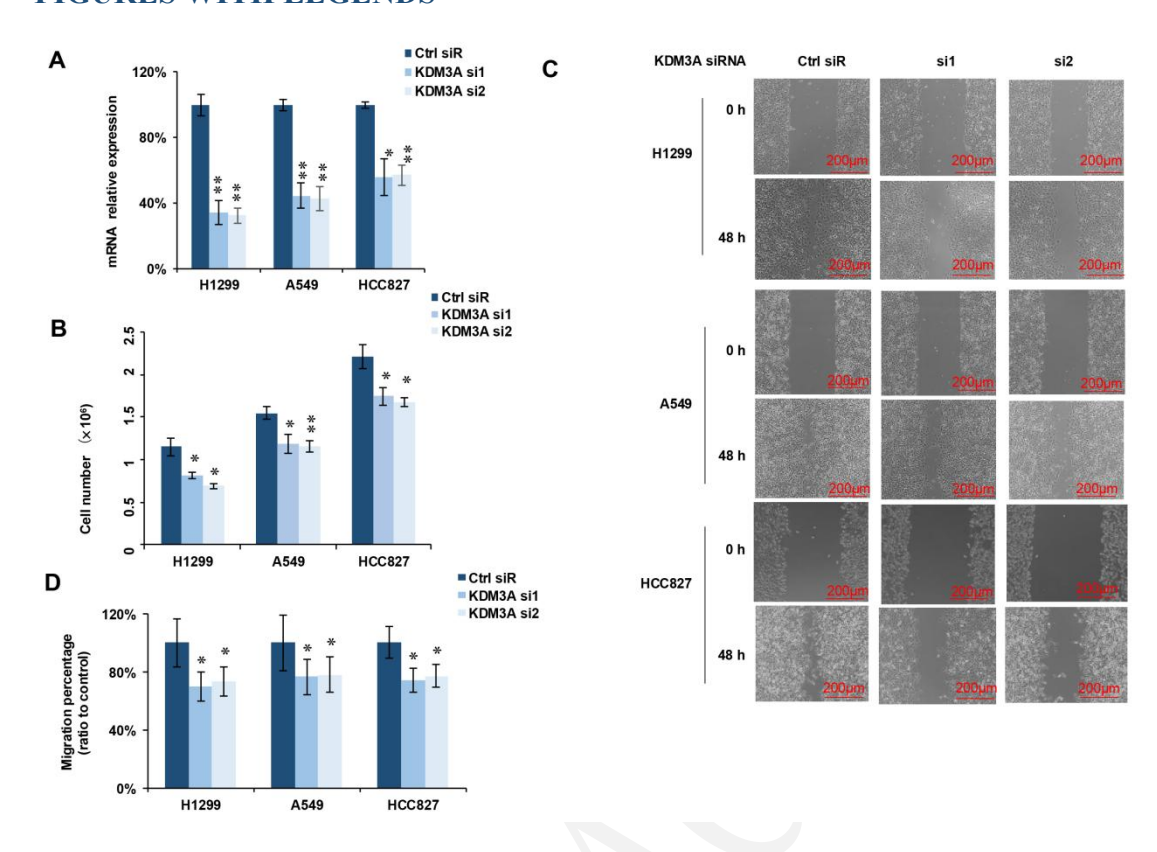


Figure 1. Knockdown of KDM3A inhibited cell proliferation and migration. (A)

Two specific KDM3A siRNAs significant down-regulated KDM3A mRNA expression in all three cells (n = 3). (B) KDM3A knockdown significantly inhibits cell proliferation in three cell lines (n = 3). (C) Wound healing assay reveals a significant decrease in migratory ability in H1299 and A549 cells following KDM3A knockdown, representative images. (D) Statistically analysis for migration distance (n = 6). Scale bar: 200µm. All the statistically analysis was conducted by Student t'test. The significance levels were displayed as follows: *, p < 0.05; **, p < 0.01; ***, p < 0.001 ns: no significant differences. Abbreviations: KDM3A: Lysine-specific demethylase 3A; siRNA: Small interfering RNA; H1299/A549/HCC827: NSCLC cell lines.

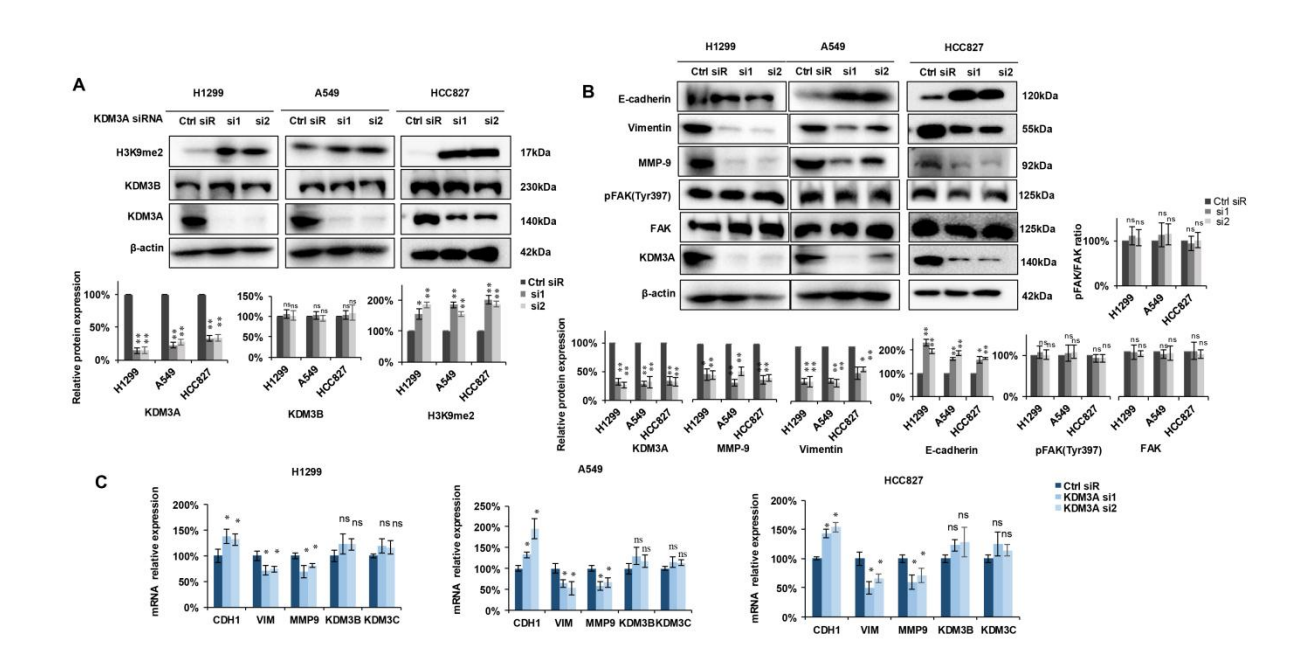


Figure 2. Knockdown of KDM3A enhanced H3K9me2 and modulated the cell invasion signaling pathway. (A) Two siRNAs inhibited KDM3A expression, leading to an upregulation of H3K9me2 in the three cells, while no significant changes for KDM3B expression. upper panel: representative blots for western blot, lower panel: statistically analysis for western blot (n = 3). (B) The expression of E-cadherin, vimentin, MMP-9, pFAK and FAK was assessed by western blotting, upper panel: representative blots for western blot, lower panel: statistically analysis for western blot (n = 3). Ratio of pFAK/FAK was calculated after normalized to the β -actin loading control, respectively. (C) The expression of E-cadherin, vimentin, MMP-9, KDM3B and KDM3C was assessed by using qRT-PCR (n = 3). The experiments were all conducted at least three times. All the statistically analysis was conducted by Student t'test. The significance levels were shown as follows: *, p < 0.05; **, p < 0.01; ***, p < 0.001, ns: no significant differences. Abbreviations: KDM3A: Lysinespecific demethylase 3A; H3K9me2: Histone H3 lysine 9 dimethylation; KDM3B: Lysine-specific demethylase 3B; KDM3C: Lysine-specific demethylase 3C; siRNA: Small interfering RNA; FAK: Focal adhesion kinase; H1299/A549/HCC827: NSCLC cell lines; VIM: Vimentin.

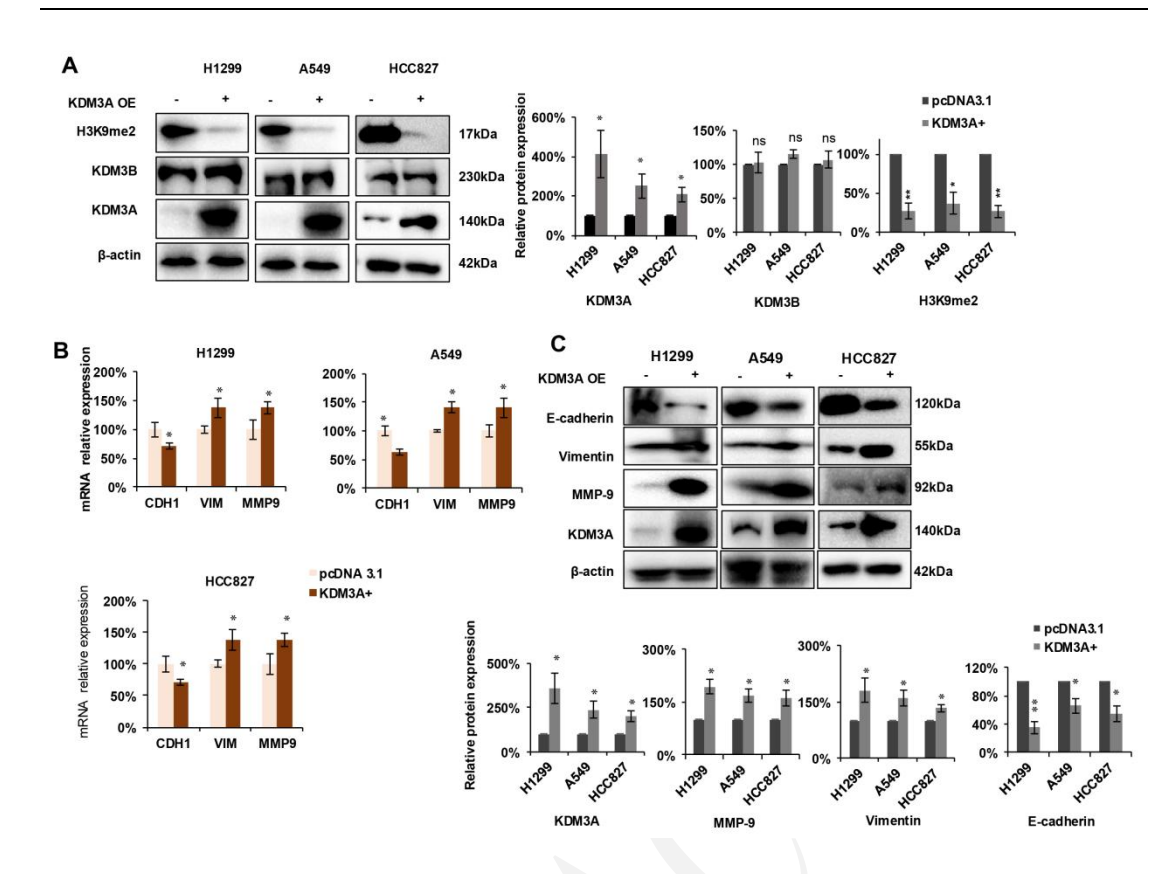


Figure 3. KDM3A overexpression up-regulated EMT and MMP-9 via regulating HeK9me2 modification of VIM and MMP-9. H3K9me2 expression decreased after KDM3A overexpression in the three cells. Left panel: representative blots for western blot, Right panel: statistically analysis for western blot (n = 3). (B) The expression of MMP-9, E-cadherin, and vimentin were assessed through qRT-PCR in three cell lines (n = 3). (C) The expression of MMP-9, E-cadherin, and vimentin were assessed through western blotting. upper panel: representative blots for western blot, lower panel: statistically analysis for western blot (n = 3). All the statistically analysis was conducted by Student t'test. The significance levels were shown as follows: *, p < 0.05; **, p < 0.01; ***, p < 0.001, ns: no significant differences. Abbreviations: KDM3A: Lysine-specific demethylase 3A; EMT: Epithelial–mesenchymal transition; H3K9me2: Histone H3 lysine 9 dimethylation; VIM: Vimentin; MMP-9/MMP9: Matrix metalloproteinase-9; E-cadherin: Epithelial cadherin.

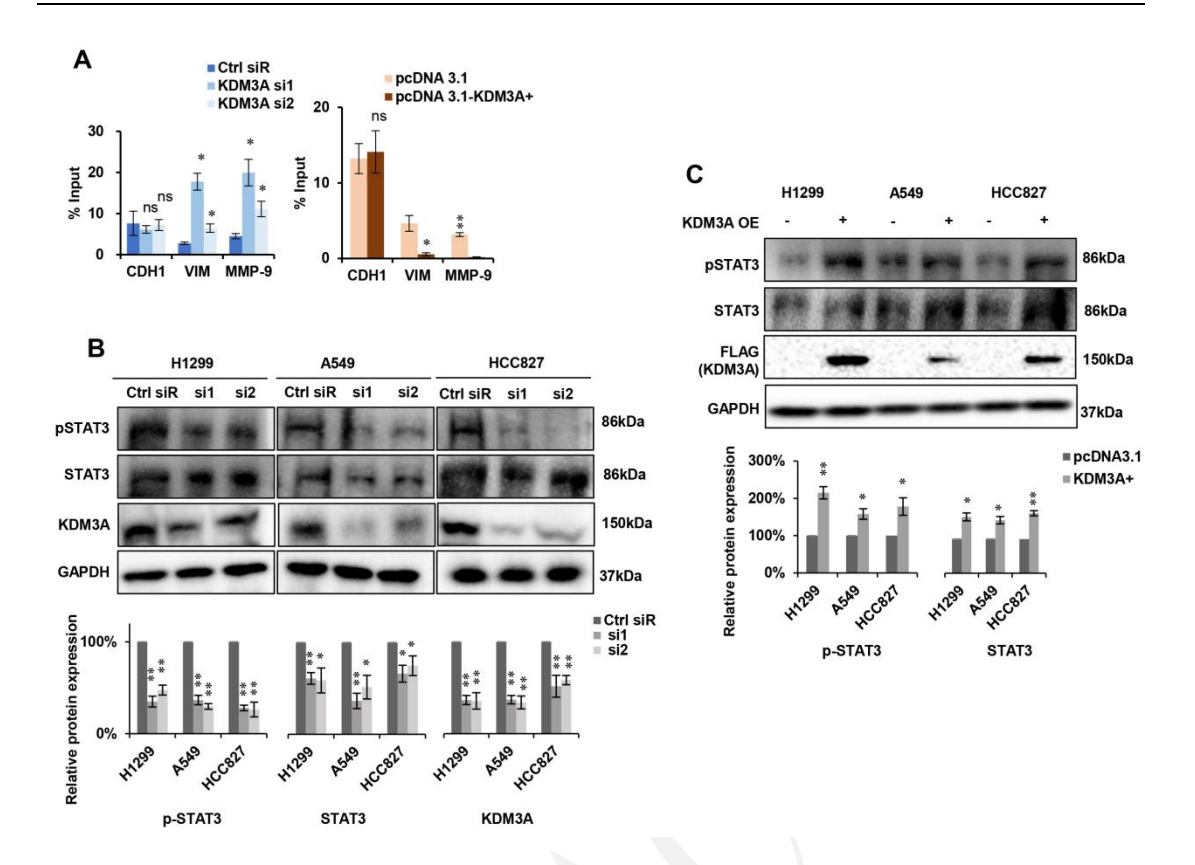


Figure 4. (A) Modulation of KDM3A regulated H3K9me2 occupancy on the promoter of VIM and MMP-9, but not CDH1. Upper panel: knockdown of KDM3A up-regulated H3K9me2 at VIM and MMP9, but not CDH1. Lower panel: over expression of KDM3A down-regulated H3K9me2 occupancy at VIM and MMP9, but CDH1 (n = 3). (B) The expression of pSTAT3, STAT3 after knocking down of KDM3A was assessed by western blotting, upper panel: representative blots for western blot, lower panel: statistically analysis for western blot (n = 3). (C) The protein expression of pSTAT3, STAT3 after overexpression of KDM3A was assessed by western blotting, upper panel: representative blots for western blot, lower panel: statistically analysis for western blot (n = 3). All the experiments were conducted at least three times. All the statistically analysis was conducted by Student t'test. The significance levels were shown as follows: *, p < 0.05; **, p < 0.01; ***, p < 0.001, ns: no significant differences. Abbreviations: KDM3A: Lysine-specific demethylase 3A; H3K9me2: Histone H3 lysine 9 dimethylation; VIM: Vimentin; MMP-9/MMP9: Matrix metalloproteinase-9; pSTAT3: Phosphorylated STAT3; STAT3: Signal transducer and activator of transcription 3.

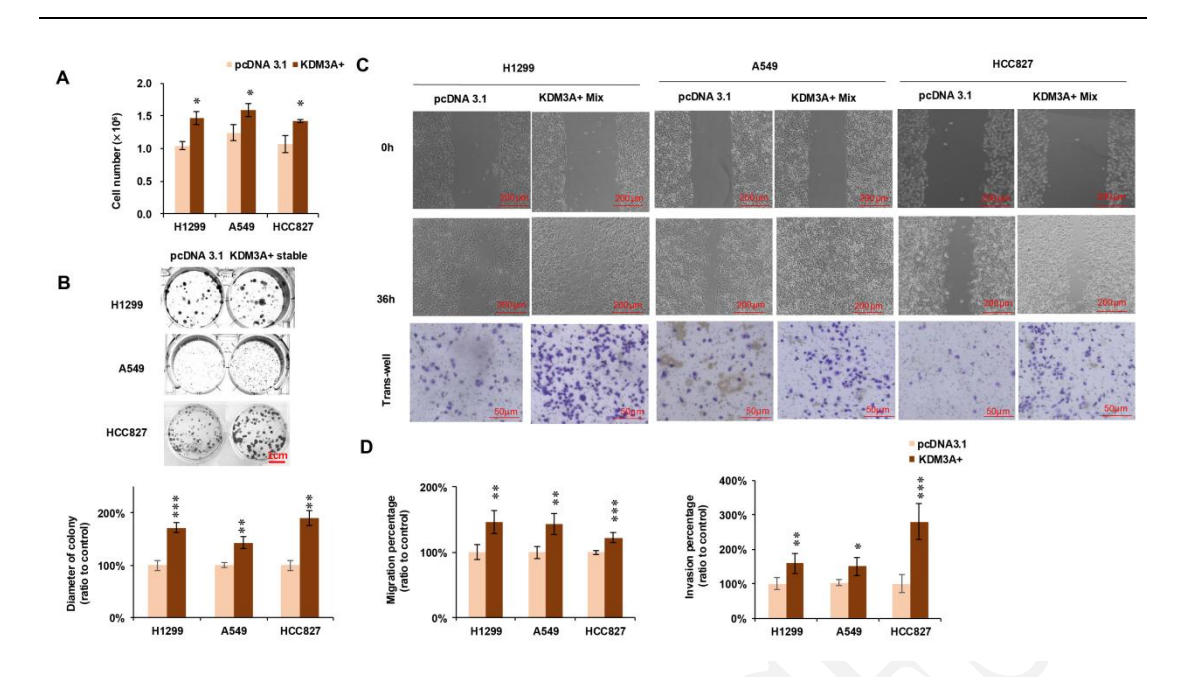


Figure 5. Overexpression of KDM3A enhances cell proliferation, migration, invasion and colony formation. (A) Cell number quantification of H1299, A549 and HCC827 after KDM3A overexpression for 72 hours (n = 3). (B) Colony formation was enhanced in H1299, A549 and HCC827 after KDM3A stably overexpression. Upper panel: representative images of cells, scale bar: 1cm. Right panel: quantification of cell clone diameters, ratio to pcDNA 3.1 control group (n = 100). (C) Upper panel: Wound healing assay assesses the migratory ability of H1299, A549 and HCC827 cells, showing a significant increase in migratory ability after KDM3A overexpression. Scale bar: 200μm. Lower panel: representative images for invasion assay, showing a significant increase in invasive ability after KDM3A overexpression. Scale bar: 50μm. (D) Quantification of migratory distance and number of invaded cells (n = 5). All the experiments were performed for at least three times and the statistically analysis was conducted by Student t'test. *, p < 0.05; **, p < 0.01; ***, p < 0.001. ns: no significant differences. Abbreviations: KDM3A: Lysine-specific demethylase 3A; H1299/A549/HCC827: NSCLC cell lines.

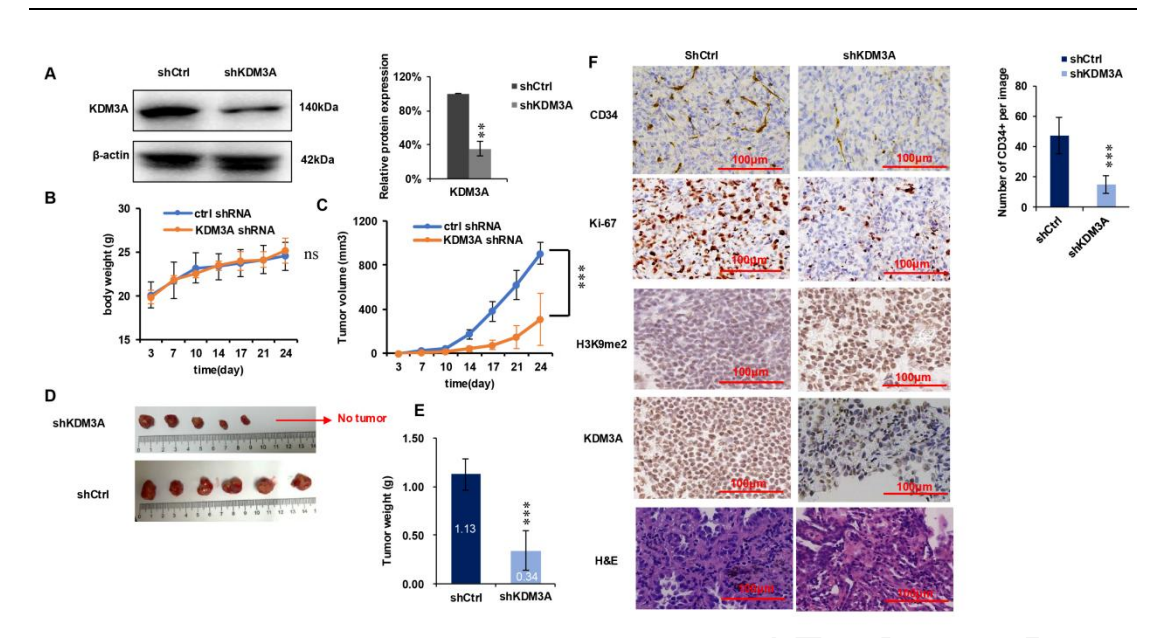


Figure 6. Knockdown of KDM3A decreased tumor formation in vivo. (A)

KDM3A were knock down stably in H1299 cells. Whole cell lysate was performed western blot. The expression of β -actin was used as loading control. Left panel: representative blots for western blot, lower panel: statistically analysis for western blot (n = 3). (B) No significant difference of body weight was observed in the two groups (n = 6, n represented for the number of mice used for each group). (C) The KDM3A knockdown group exhibited lower tumor growth speed comparing with the control group. Tumor growth was monitored twice a week. Tumor volume was calculated by $0.5 \times L \times W^2$ (n = 6, n represents for the number of mice used for each group). (D) Images of tumor samples of shCtrl and shKDM3A group. (E) Tumor weight quantification for shCtrl and shKDM3A group (n = 6, n represents for the number of mice used for each group). (F) Left panel: representative images for HE staining and Immunohistochemical staining of KDM3A, H3K9me2, KI67 and CD34 for tumor tissues, scale bar: 100 µm. Right panel: micro-vessel quantification based on CD34 IHC staining. (n = 12, n represents for the number of images for each group, 2 images per mouse was used). All the statistically analysis was conducted by Student t'test. The significance levels were shown as follows: *, p < 0.05; **, p < 0.01; ***, p < 0.001. ns: no significant differences. Abbreviations: KDM3A: Lysinespecific demethylase 3A; H1299: NSCLC cell line; H3K9me2: Histone H3 lysine 9 dimethylation; HE: Hematoxylin–eosin; Ki-67/KI67: Proliferation marker Ki-67.

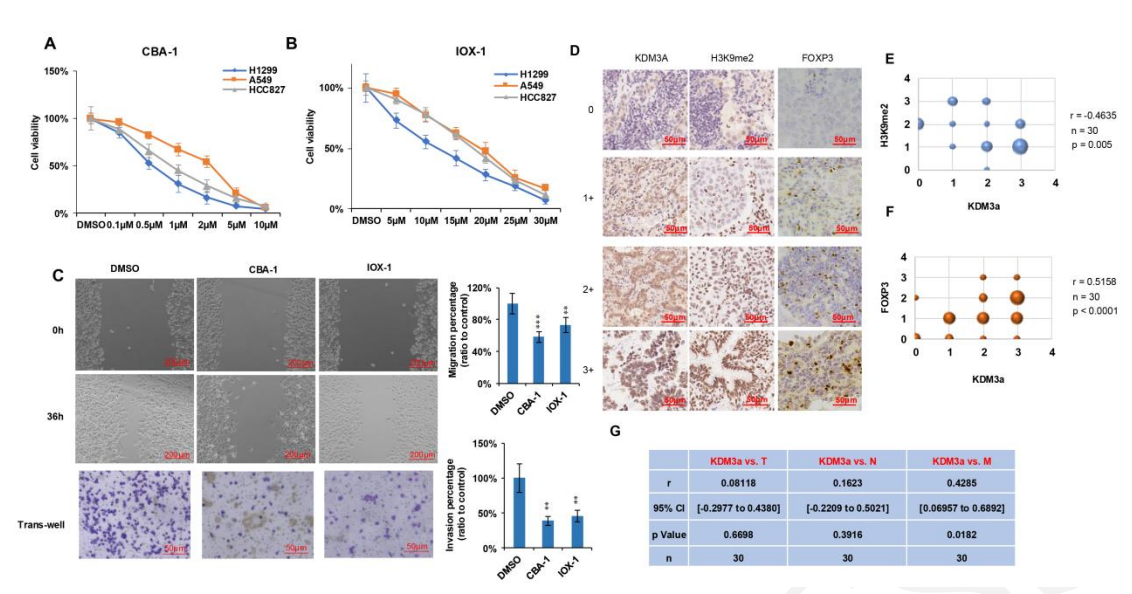


Figure 7. KDM3A is a potential therapeutic target for NSCLC. (A and B)

KDM3A inhibitor CBA-1 and IOX-1 inhibited cell viability of all the three NSCLC cells (n = 5). (C) CBA-1 and IOX-1 inhibited cell migration and invasion of H1299. H1299 was treated with CBA-1 or IOX-1 and performed wound healing assay to evaluate the migratory ability or trans-well assay to evaluate the invasive ability. Left panel: representative image of cells. Right panel: statistically analysis for migration distance and invasion percentage. The statistically analysis was conducted by Student t'test (n = 5). (D) IHC score of KDM3A, H3K9me2 and FOXP3 of clinical patient samples. Scale bar: 100 µm. (E) Spearman correlation between KDM3A and H3K9me2 IHC score (n = 30). (F) Spearman correlation between KDM3A and FOXP3 IHC score (n = 30). (G) Spearman correlation between KDM3A and TNM stage (n = 30). The significance levels were shown as follows: *, p < 0.05; **, p < 0.01; ***, p < 0.001. Abbreviations: KDM3A: Lysine-specific demethylase 3A; NSCLC: Non-small cell lung cancer; CBA-1: Small-molecule KDM inhibitor; H1299/A549/HCC827: NSCLC cell lines; H3K9me2: Histone H3 lysine 9 dimethylation.

SUPPLEMENTAL DATA

Supplementary figures

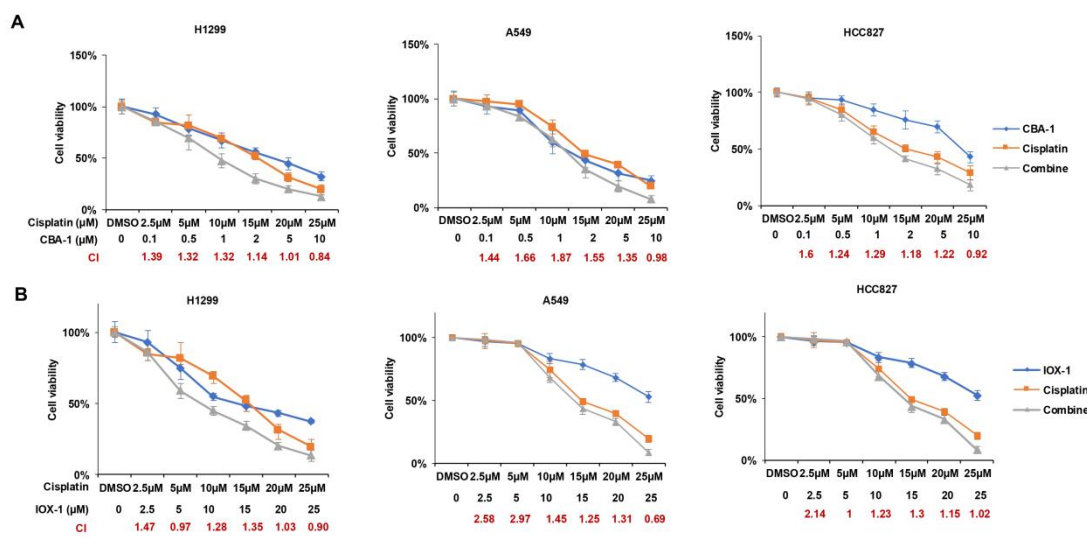


Figure S1. Combination therapy of KDM3A and cisplatin treatment showed no synergistic inhibitor for NSCLC *in vitro*. (A) Cell viability of the three cell lines after treating with CBA-1, cisplatin alone or combination at indicated concentrations (n = 5). (B) Cell viability of the three cell lines after treating with IOX-1, cisplatin alone or combination at indicated concentrations (n = 5). Abbreviations: KDM3A: Lysine-specific demethylase 3A; NSCLC: Non-small cell lung cancer; CBA-1: Small-molecule KDM inhibitor; IOX-1: Broad-spectrum KDM inhibitor; H1299/A549/HCC827: NSCLC cell lines.